Crystallographic Investigation of the Role of Aspartate 95 in the Modulation of the Redox Potentials of *Desulfovibrio vulgaris* Flavodoxin[†,‡]

Andrew A. McCarthy,[§,||] Martin A. Walsh,[*,⊥,@] Chandra S. Verma,[#] David P. O'Connell,[+,○] Meike Reinhold,[#] Gary N. Yalloway,[+,◇] Darren d'Arcy,[§] Timothy M. Higgins,[§] Gerrit Voordouw,[●] and Stephen G. Mayhew[+]

Department of Chemistry, National University of Ireland, Galway, Ireland, European Molecular Biology Laboratory, c/o DESY, Notkestrasse 85, D-22603 Hamburg, Germany, York Structural Biology Laboratory, Department of Chemistry, University of York, Heslington YO10 5DD, U.K., Department of Biochemistry, University College Dublin, Dublin 4, Ireland, and Department of Biological Sciences, University of Calgary, Calgary, Alberta, Canada

Received March 21, 2002; Revised Manuscript Received June 24, 2002

ABSTRACT: The side chain of aspartate 95 in flavodoxin from *Desulfovibrio vulgaris* provides the closest negative charge to N(1) of the bound FMN in the protein. Site-directed mutagenesis was used to substitute alanine, asparagine, or glutamate for this amino acid to assess the effect of this charge on the semiquinone/hydroquinone redox potential (E_1) of the FMN cofactor. The D95A mutation shifts the E_1 redox potential positively by 16 mV, while a negative shift of 23 mV occurs in the oxidized/semiquinone midpoint redox potential (E_2). The crystal structures of the oxidized and semiquinone forms of this mutant are similar to the corresponding states of the wild-type protein. In contrast to the wild-type protein, a further change in structure occurs in the D95A mutant in the hydroquinone form. The side chain of Y98 flips into an energetically more favorable edge-to-face interaction with the bound FMN. Analysis of the structural changes in the D95A mutant, taking into account electrostatic interactions at the FMN binding site, suggests that the $\pi-\pi$ electrostatic repulsions have only a minor contribution to the very low E_1 redox potential of the FMN cofactor when bound to apoflavodoxin. Substitution of D95 with glutamate causes only a slight perturbation of the two one-electron redox potentials of the FMN cofactor. The structure of the D95E mutant reveals a large movement of the 60-loop (residues 60−64) away from the flavin in the oxidized structure. Reduction of this mutant to the hydroquinone causes the conformation of the 60-loop to revert back to that occurring in the structures of the wild-type protein. The crystal structures of the D95E mutant imply that electrostatic repulsion between a carboxylate on the side chain at position 95 and the phenol ring of Y98 prevents rotation of the Y98 side chain to a more energetically favorable conformation as occurs in the D95A mutant. Replacement of D95 with asparagine has no effect on E_2 but causes E_1 to change by 45 mV. The D95N mutant failed to crystallize. The K_d values of the protein FMN complex in all three oxidation−reduction states differ from those of the wild-type complexes. Molecular modeling showed that the conformational energy of the protein changes with the redox state, in qualitative agreement with the observed changes in K_d, and allowed the electrostatic interactions between the FMN and the surrounding groups on the protein to be quantified.

Flavodoxins are a group of small flavoproteins (molecular masses of 14000−23000 Da) that have been isolated from a wide range of microorganisms. They are the smallest members of the flavoprotein family. They contain a single molecule of flavin mononucleotide (FMN),[1] and they function as electron carriers in low-potential oxidation−reduction reactions, such as nitrogen fixation and photosynthesis, in which they transfer electrons between other redox proteins. In some organisms, they are synthesized in place of ferredoxin in response to iron deficiency. They have been studied intensively, and several comprehensive reviews on their

[†] This work was supported in part by grants from BioResearch Ireland. M.A.W. was supported by an EU Institutional Fellowship contract (CT 930485). C.S.V. thanks the BBSRC for support.

[‡] Atomic coordinates and structure factors for the structures described in this work have been deposited in the Protein Data Bank: 1AKQ for D95A ox, 1AKV for D95A sq, 1AKU for D95A hq, 1C7F for D95E ox, and 1C7E for D95E hq.

* To whom correspondence should be addressed: Medical Research Council, c/o ESRF, BP 220, 38043 Grenoble Cedex, France. E-mail: walsh@esrf.fr. Telephone: +33-4-7688-2380. Fax: +33-4-7688-2380.

[§] National University of Ireland.

[||] Present address: European Molecular Biology Laboratory (EMBL), 6, rue Jules Horowitz, BP181, 38042 Grenoble Cedex 9, France.

[⊥] European Molecular Biology Laboratory.

[@] Present address: Medical Research Council (MRC), c/o ESRF BP 220, 38043 Grenoble Cedex, France.

[#] University of York.

[+] University College Dublin.

[○] Present address: Trends in Microbiology, 84 Theobalds Rd., London WC1X 8RR, U.K.

[◇] Present address: Institut für Biophysikalische Chemie, Johann Wolfgang Goethe-Universität Biozentrum N230, Marie Curie-Strasse 9, 60439 Frankfurt am Main, Germany.

[●] University of Calgary.

[1] Abbreviations: SRS, synchrotron radiation source; DESY, Deutsches Elektronen-Synchrotron; rms, root-mean-square; FMN, flavin mononucleotide; EDTA, ethylenediaminetetraacetic acid; E_1, midpoint potential for the semiquinone/hydroquinone couple; E_2, midpoint potential for the oxidized/semiquinone couple; ox, oxidized; sq, semiquinone; hq, hydroquinone; wt, wild type.

10.1021/bi020225h CCC: $22.00
Published on Web 08/13/2002

structure and function have appeared (*1*−*3*). The flavodoxins continue to attract interest because of the dramatic changes that occur in the redox properties of FMN when the flavin is bound to the apoprotein, because the interactions responsible for these changes are not yet fully understood, and because flavodoxin-like domains occur in much larger proteins. FMN can accept two electrons and can exist in three oxidation states: oxidized (ox), semiquinone (sq), and hydroquinone (hq). Interactions between the bound FMN and apoprotein perturb the two one-electron redox potentials; the midpoint potential at pH 7 of the oxidized/semiquinone couple (E_2) is shifted positively by 60−180 mV (1.4−4.2 kcal/mol), and the midpoint potential of the semiquinone/hydroquinone couple (E_1) is shifted negatively by at least 200 mV (>4.6 kcal/mol).

Three-dimensional structures have been determined for oxidized flavodoxins from the bacteria *Clostridium beijerinckii* MP (*4*), *Megasphaera elsdenii* (*5*, *6*), *Desulfovibrio vulgaris* (*7*), *Anacystis nidulans* (*8*), *Escherichia coli* (*9*), *Anabaena variabilis* (*10*), and *Desulfovibrio desulfuricans* (*11*) and from the alga *Chondrus crispus* (*12*). Structural comparisons of the oxidized form with semiquinone and/or hydroquinone forms are available for the flavodoxins from *C. beijerinckii* MP (*13*, *14*), *M. elsdenii* (*5*, *6*), *D. vulgaris* (*7*), and *A. nidulans* (*15*). The structures of the flavodoxins for which all three oxidation states have been elucidated show that a general trend on reduction to the semiquinone state involves a peptide flip at a glycine residue which allows a hydrogen bond to form between the carbonyl oxygen of the glycine and the N(5)H group of the reduced FMN (*5*, *7*, *13*, *15*). This new interaction is believed to contribute to the stabilization of the flavin semiquinone. A proposal that the ox/sq redox potential of *C. beijerinckii* MP flavodoxin is modulated by changes in the protein−FMN interactions and by changes in the conformational energy of the protein itself (*16*) has recently been confirmed experimentally (17).

D. vulgaris and *C. beijerinckii* MP flavodoxins undergo no further changes in structure when they are reduced from the semiquinone to the hydroquinone (*7*, *14*), and thus, the large negative shift in the E_1 redox potential has been more difficult to rationalize. Initially, it was thought that the free flavin hydroquinone is not planar and that the planarity of the dimethylisoalloxazine structure when bound to apoflavodoxin observed in the X-ray crystal structures is enforced by the protein and thus contributes to the destabilization of this oxidation state. However, NMR studies suggest that the hydroquinone of free flavin is also close to planar (*18*). Uncertainty still remains because recent theoretical calculations suggest that the neutral hydroquinone of free flavin is in fact bent along the N(5)−N(10) axis with a puckering angle of 25−27° but with a low energy barrier to inversion [<6.5 kcal/mol (*19*, *20*)].

Ludwig et al. (*21*) have provided evidence from the properties and X-ray crystallographic structure of the protein complex with 1-deaza-FMN that protonation at N(1) is sterically restricted in *C. beijerinckii* MP flavodoxin. This has been further substantiated by NMR measurements on *M. elsdenii* (*22*) and *D. vulgaris* (*23*) flavodoxins which have indicated that the flavin hydroquinone is bound as an anion with the negative charge at N(1). Therefore, recent research has concentrated on the importance of charge interactions at the FMN binding site in contributing to the destabilization of the hydroquinone form. A number of general features in the structure of the FMN binding sites of flavodoxins have strengthened the idea that electrostatic interactions between the negatively charged hydroquinone of FMN and the protein play an important part in the modulation of the E_1 redox potential (*24*−*28*).

Three major sources of unfavorable electrostatic interactions with this negatively charged hydroquinone form have been singled out. First, the isoalloxazine system is usually found in a very apolar environment, typically sandwiched between aromatic hydrophobic amino acid side chains. In the case of *D. vulgaris* flavodoxin, a tryptophan (W60) flanks the inner or *re*-face of the isoalloxazine and tyrosine (Y98) flanks the outer or *si*-face. Y98 is nearly coplanar with the isoalloxazine system, and W60 makes an angle of approximately 45°. Second, a high concentration of charged acidic amino acids in the proximity of the FMN binding site further hinders the formation of a negatively charged flavin hydroquinone. Finally, the phosphate-binding site of the 5′-phosphate of FMN consists primarily of serine and threonine residues, and hydrogen-bonding interactions predominate. The dianionic charge on the phosphate is not offset in this highly conserved phosphate-binding site, and it has been suggested (*28*) that the negative charge on the phosphate could contribute to the modulation of the E_1 redox potential through unfavorable electrostatic interactions with the charge at N(1). Studies by Zhou and Swenson (*26*) and Walsh et al. (*29*) have allowed the conclusion that this interaction can have only a small effect. The combination of all these features makes it difficult to form the negatively charged hydroquinone of flavodoxins, and this is reflected in the large negative shift of the E_1 redox potential of the bound flavin. It should be noted, however, that although the flavin hydroquinone in flavodoxins does not protonate in the pH region in which free FMN hydroquinone protonates (pK_a = 6.7), the optical spectrum of this redox form of the bound flavin changes with pH (*30*) as do the ^{13}C and ^{15}N NMR spectra of *D. vulgaris* flavodoxin (*31*).

Other important factors which may contribute to destabilization of the hydroquinone include aromatic stacking interactions and solvent exclusion at the FMN binding site (*24*, *27*). Both of these factors in *D. vulgaris* flavodoxin are largely controlled by the tyrosine residue, which is nearly coplanar to the *si*-face of the isoalloxazine. In the most recent study (*27*), Y98 was mutated to an alanine and the six negatively charged side chains that are closest to N(1) of the flavin were neutralized. The redox potential of this mutant is shifted much closer to that of free FMN. This supports the view that the value of E_1 in flavodoxin results largely from the cumulative effect of unfavorable electrostatic interactions introduced by coplanar aromatic stacking between Y98 and the negatively charged flavin hydroquinone, and the negative electrostatic environment of the FMN binding site. The side chain of D95 provides the closest negative charge to flavin N(1) of *D. vulgaris* flavodoxin (∼6 Å), and its backbone also provides hydrogen bonding interactions to N(1) and O(2) of the flavin. Neutralization of this acidic side chain results in a positive shift in E_1 that is larger than the one that occurs when other acidic side chains in the vicinity of the FMN binding site are neutralized (*25*). This result and others (*32*) suggest that D95 in *D. vulgaris* flavodoxin may have a special role in regulating

Table 1: Data Collection and Reduction Statistics

	D95A ox	D95A sq	D95A hq	D95E ox	D95A hq
wavelength λ (Å)	0.962	0.9	0.937	1.54	1.54
temperature (K)	293	100	100	293	100
space group	$P4_32_12$	$P4_32_12$	$P4_32_12$	$C2$	$C2$
unit cell					
a (Å)	52.81	52.61	52.56	94.32	93.04
b (Å)	52.81	52.61	52.56	61.93	61.51
c (Å)	139.95	138.34	140.26	74.21	75.55
α, β, γ (deg)	90, 90, 90	90, 90, 90	90, 90, 90	90, 127.16, 90	90, 127.06, 90
maximum resolution (Å)	1.83	1.96	1.9	2.0	2.25
total no. of full observations	70384	49473	47870	52226	35676
no. of unique observations	17939	13307	16098	19635	15535
completeness (%)[a]	98 (97.6)	99.5 (96.5)	98.9 (99)	94.1 (91.9)	95.4 (92.9)
R_{merge} (%)[a,b]	5.2 (29.8)	4.4 (33.7)	4.2 (32.1)	6.1 (22.4)	6.6 (31.4)

[a] Values in parentheses are for the highest-resolution shell.

[b] $R_{merge} = \sum_{hkl}\sum_{i=1}^{N}|\langle I^{hkl}\rangle - I_i^{hkl}|/\sum_{hkl}\sum_{i=1}^{N} I_i^{hkl}$.

E_1. In this paper, we describe the structures of the various oxidation states of the *D. vulgaris* flavodoxin mutants D95A and D95E. Calculation of the charge interactions at the FMN binding site for all these structures has allowed new insights into the role of electrostatic interactions in the modulation of the bound FMN's redox potentials to be gained. The structures highlight the importance of the hydrogen bonding network in the modulation of the bound FMN's redox potentials, in which the carboxylate group of D95 plays a key role.

MATERIALS AND METHODS

Mutagenesis, Purification, and Characterization of Proteins. The methods used to obtain the genes for the three mutant flavodoxins, to express the genes in *E. coli*, to purify the proteins, and to characterize them biochemically were as described previously (*33*).

Crystallization and Preparation of Reduced Crystals. Crystals of the D95A mutant protein were grown by the hanging- or sitting-drop vapor diffusion methods, using protein solutions of 12−15 mg/mL and 30−35% saturated ammonium sulfate buffered to pH 7.0 with either 50 mM Tris-HCl or 25 mM sodium phosphate containing 1 mM EDTA at 18 °C and over a solution of 60−70% saturated ammonium sulfate. Crystals develop as well-formed, elongated, yellow tetragonal bipyramids with a major dimension of 0.8−1.3 mm after growth for approximately 1 month. The crystals of the D95A mutant belong to space group $P4_32_12$ with one molecule in the asymmetric unit, similar to the wild-type flavodoxin (*7*, *34*). The D95E mutant protein was crystallized at 18 °C, using the hanging-drop vapor diffusion method. The crystals formed as flat plates from drops containing 12−15 mg/mL protein and equilibrated against 70−73% saturated ammonium sulfate, 200 mM Tris-HCl (pH 8.5), and 200 mM sodium acetate. Small plates were used as macroseeds to develop crystals large enough for data collection. The crystals belong to space group $C2$, and they contain two molecules in the asymmetric unit.

Oxidized crystals of D95A and D95E flavodoxin were reduced chemically using sodium dithionite. The reductions of the crystals were carried out in an anaerobic environment. The following protocol was used for full reduction of the crystals. Crystals were first transferred to a deaerated stabilizing solution (80% saturated ammonium sulfate and 14% glycerol buffered to pH 8.5 with 100 mM Tris-HCl). A solution of the stabilizing buffer containing sodium dithionite (8 mg/mL) was then slowly added to these crystals until the dithionite was in excess. The reduction was followed by the color change. Initially, the crystals take on a reddish color due to the semiquinone and then they gradually turn to the light straw yellow color of the hydroquinone. The reducing power of sodium dithionite depends on pH, and an excess of the reducing agent at pH 6 reduces the flavodoxin only to its semiquinone form (*35*). Hence, the semireduced form can be obtained by carrying out the above reduction procedure in stabilizing solutions of 80% ammonium sulfate and 14% glycerol buffered to pH 6 with 50 mM sodium phosphate. The crystals slowly changed from yellow to a reddish color over a period of 15−20 min using these conditions. Attempts to crystallize the D95N mutant from solutions of oxidized or reduced protein thus far have been unsuccessful.

Data Collection and Reduction. X-ray diffraction data for the oxidized form of the D95A mutant were collected on a Mar-Research imaging plate using synchrotron radiation from station PX9.5, SRS (Daresbury, U.K.). The crystal was mounted with the C^* axis collinear with the spindle axis of the camera. Twenty-eight degrees were collected in 1.5° oscillations/frame with an exposure time of 50 s per degree. A further 30° of data were collected with an oscillation range of 2°/frame and an exposure time of 60 s per degree. X-ray diffraction data were collected on Mar-Research imaging plate detectors using synchrotron radiation from EMBL beamlines X11 and X31 at the DORIS storage ring (DESY, Hamburg, Germany) for the D95A semiquinone and D95A hydroquinone. The data for the oxidized D95E mutant and for the hydroquinone of the D95E mutant were collected on a Rigaku R-axis II imaging plate using a Rigaku RU-200 X-ray generator operating at 50 kV and 94 mA, equipped with a copper anode ($\lambda = 1.54$ Å) and Molecular Structure Corp. double-focusing mirrors. Each data set was integrated, scaled, and merged using the programs DENZO and SCALEPACK (*36*), respectively. Table 1 contains a summary of the data collection and reduction statistics.

Structure Solution and Refinement. The coordinates of the oxidized wild-type protein (*34*) were positioned in the D95A

Table 2: Refinement Statistics

	D95A			D95E	
	ox	sq	hq	ox	hq
resolution range (Å)	10−1.9	10−2	12−1.9	12−2.0	12−2.25
R^a	19.6	20.1	21.5	17.97	23.08
free R^b	23.63	25.71	27.91	23.79	29.4
no. of atoms (non-hydrogen)					
total	1232	1288	1297	2423	2411
protein	1101	1101	1101	2210	2210
FMN	31	31	31	31	31
water	100	137	155	151	139
sulfate ions	−	1	−	−	−
rmsd from ideal geometry (Å)					
bond distance (1−2)	0.01	0.014	0.019	0.015	0.022
bond distance (1−3)	0.031	0.033	0.039	0.034	0.047
bond distance (1−4)	0.034	0.035	0.042	0.035	0.049
mean displacement parameters (Å^2)					
all atoms	21.2	18.4	23.2	31.6	43.0
protein atoms	19.8	16.9	21.7	31.1	43.0
FMN atoms	12.2	11.0	14.9	22.1	33.5
solvent atoms	39.4	29.7	33.6	43.0	47.7

[a] $R = 100\sum_h|F_o - F_c|/\sum_h|F_o|$. [b] Cross-validation *R*-factor calculated by omitting 5% of the reflections during refinement (*69*).

oxidized, semiquinone, and hydroquinone unit cells by rigid body refinement with AMoRe (*37*). The structures were refined by iterative cycles of $2F_o - F_c$ and $F_o - F_c$ electron density map inspection with O (*38*) and restrained least-squares refinement with the program PROLSQ, as implemented in the CCP4 suite (*39*), coupled with ARP (*40*). All solvent molecules were refined with unit occupancy. In addition, the solvent molecules were visually inspected, and they were deleted if they were not within hydrogen bonding distance of one or more potential hydrogen bond partners, and if they were close to regions in which the protein density was ambiguous. Refinement statistics are compiled in Table 2.

The D95E mutant crystallizes with two molecules per asymmetric unit in space group *C*2. The mutant structure was determined by molecular replacement using AMoRe (*37*). Refinement was carried out using a protocol similar to that for the D95A mutant data. Regions of the structure that differed significantly from the refined wild-type coordinates were rebuilt in O (*38*) with the aid of omit maps. These maps were calculated after five cycles of refinement with REFMAC (*39*) where the region of the structure in question had been omitted. In this way, electron density maps with minimized model bias were produced. Further iterative cycles of refinement and manual inspection of $2F_o - F_c$ and $F_o - F_c$ electron density maps with the addition of waters to the model were performed until convergence (Table 2).

Molecular Modeling. The protein−ligand systems were represented by the polar atom CHARMM22 force field (*41*) using protocols outlined elsewhere (*42*). In this model, the aromatic rings, with hydrogen atoms represented explicitly, are modeled such that quadrupole interactions, which incorporate the excess negative charges on either faces, are included. To determine the point charges for FMN in all of its oxidation states, single-point calculations were carried out utilizing density functional theory [Amsterdam Density Functional Program (*43*−*49*)], parametrized by Vosko, Wilk, and Nusair (*47*). Gradient corrections by Becke (*48*) and correlation corrections by Lee, Yang, and Parr were applied (*49*). Double-ζ basis sets with additional polarization functions have been used. The frozen core approximation was applied for carbon, nitrogen, oxygen (all 1s), and phosphorus (2p). Calculations were performed without incorporating any symmetry. Unrestricted calculations have been carried out for neutral and anionic hydroquinone. The point charges were calculated using Mulliken's population analysis. These calculations differ somewhat from the extensive calculations that have been used to derive the charges for amino acids (*50*). However, this does not pose a problem because the charges of the flavin moiety in all three oxidation states have all been calculated in a self-consistent manner and we are concerned only with the relative differences in interaction between the amino acids and the three oxidation states of the flavin. The nonbonded interactions were truncated at 14 Å with the electrostatics shifted to 0 at 12 Å and the van der Waals interactions switched between 8 and 12 Å. Nonbonded energies of interaction between each residue in the proteins (native and two mutants, D95A and D95E) were calculated with the dielectric represented by scaling down the electrostatic interactions with a factor of 5. All calculations were performed using Charmm, version 27, while the electrostatic free energies of binding (these are free energies since the solvent is modeled as a continuum representing an average over multiple conformations) were calculated from the finite-difference solutions of the linearized Poisson−Boltzmann equation using the program UHBD [version 6.1 (*51*−*55*)]. The protein was treated as a region with a relatively low dielectric constant (values of 1, 2, 10, and 20 were examined), and the solvent, which was modeled as a continuum, was assigned a dielectric of 78. Charges and atomic radii were assigned from the same parameter sets that were used above. An ionic concentration of 50 mM at 300 K was used to simulate the conditions used in the experiments.

RESULTS

Biochemical Properties of Mutant Flavodoxins. The optical spectra of the three redox forms of the D95A, D95E, and D95N mutant flavodoxins are similar to those of the wild-type protein (*56*). Similarly, addition of one electron to each of the proteins gives the neutral form of the FMN semiquinone, and addition of a second electron produces the

Table 3: Thermodynamic Properties of *D. vulgaris* Wild-Type, D95A, and D95E Flavodoxins[a]

	dissociation constant (nM)			redox potential (mV)		redox-linked
	ox	sq	hq	ox/sq	sq/hq	pK_a
wild type[b]	0.24	0.00032	173	−143	−440	7.0
D95A[c]	0.79	0.0026	746	−166	−424	6.5
D95E	0.30	0.00066	505	−156	−449	
D95N	1.1	0.0016	150	−145	−395	5.6
				−176[e]	−397[e]	
FMN[d]				−313	−101	

[a] The data were obtained at 20 (FMN) or 25 °C (proteins) and are reported for pH 7. [b] From refs *56* and *58*. [c] From ref *32*. [d] From refs *57* and *58*. [e] From ref *25*.

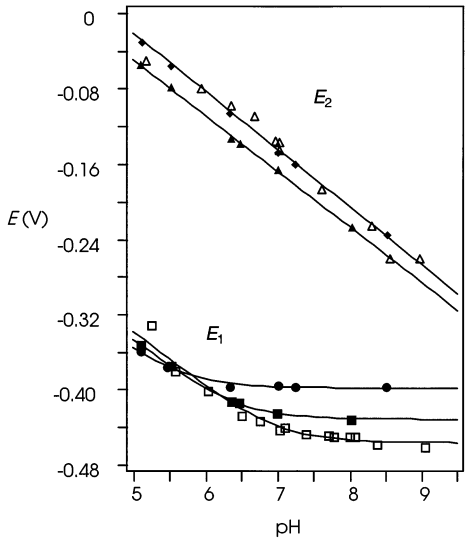

FIGURE 1: Effects of pH on the midpoint oxidation−reduction potentials of wild-type flavodoxin and the D95A mutants. Redox potentials were determined by potentiometry (*33*, *56*). The empty symbols represent data points for the wild-type protein and are taken from ref *56*. The filled symbols are for the mutants: (◆ and ▲) potentials of the oxidized/semiquinone couple (E_2) for D95N and D95A, respectively, and (■ and ●) potentials of the semiquinone/hydroquinone couple (E_1) for D95N and D95A, respectively. The lines drawn through the values for E_1 are theoretical lines for a one-electron redox system in which the reductant has a pK_a of 7.0 (wild type), 6.5 (D95A), or 5.6 (D95N).

hydroquinone. The midpoint oxidation−reduction potentials of the two one-electron steps in reduction of the mutant proteins were determined by potentiometry (Table 3 and Figure 1). Removal of the negative charge closest to N(1) of the bound flavin causes a small convergence of the two redox potentials, resulting in a slight destabilization of the semiquinone. In the case of the D95A mutant, the potentials of both steps change; in contrast, the E_2 potential for the D95N mutant is unchanged, while the E_1 potential becomes 45 mV less negative. The stabilities of the semiquinone forms of the D95A and D95N mutants, as determined from the differences between the potentials of the two steps in reduction, are therefore very similar. The effects of pH on the potentials of the D95A and D95N mutants were investigated (Figure 1). The two potentials vary with pH in a manner similar to that of the corresponding potentials for wild-type flavodoxin (*56*). The slope, ΔE_2/pH, is -60 ± 1 mV between pH 5.1 and 9.0, consistent with the addition of an electron and a proton to the oxidized flavin in forming the semiquinone. In contrast, the values for E_1 are independent of pH at high pH but become pH-dependent at low pH. The change in slope suggests that the fully reduced forms of the flavoproteins undergo a protonation step that does not occur in the semiquinone. The pK_a value for this apparent protonation step decreases as the values for E_1 become less negative (Table 3).

The strength of the interaction of oxidized FMN with the D95E mutant is very similar to that of wild-type flavodoxin, as reflected in the dissociation constant, while the other two mutant apoproteins seem to bind FMN somewhat less strongly (Table 3). The very strong binding of FMN by all of the proteins means that it is difficult to determine K_d values with high precision even using the quenching of FMN fluorescence to monitor the interaction (*56*). However, the apoprotein of *D. vulgaris* flavodoxin also binds riboflavin. The interaction with this flavin is much weaker than the interaction with FMN, and K_d values can therefore be determined, by either fluorescence or light absorbance measurements, with much greater confidence. The values determined for the complexes with riboflavin are 0.72 μM for the wild-type protein (*56*) and 7.3 and 40 μM for the D95A and D95N mutant proteins, respectively. These values make it clear that although the two mutations have a greater effect on riboflavin binding than on FMN binding, the order and direction of the change are the same for the complexes with both flavins. Use of the dissociation constants for the complexes with FMN and the two redox potentials for FMN in the free form (*57*, *58*) and bound to the proteins allows values for the dissociation constants for the protein complexes with the semiquinone and hydroquinone of FMN to be calculated (*56*). The calculations show that the greatest difference from the wild-type flavodoxin occurs with the semiquinone complex of the D95A mutant, which is about 8 times weaker than the corresponding complex of the wild-type protein (Table 3). The strength of the interaction of the hydroquinone of FMN with the D95N mutant apoprotein is about the same as that of the wild-type protein.

Quality of the Structures. The models of the oxidized, semiquinone, and hydroquinone forms of the D95A mutant show excellent fits to the corresponding $2F_o - F_c$ electron density maps (Figure 2). Only a few surface glutamine and lysine side chains could not be modeled, as was also observed with wild-type flavodoxin (*7*, *34*). Ramachandran plots (*59*) for the main chain dihedral angles showed that 99.2% of the oxidized form of the D95A mutant and all of the residues in both the semiquinone and hydroquinone forms of the mutant (excluding glycine residues) have dihedral angles that fall in or near the energetically preferred regions. Only D62 of the oxidized D95A mutant structure falls outside this region, as was also seen in wild-type flavodoxin. D62 is part of a reverse turn and is involved in FMN binding, and the electron density unambiguously defines this conformation. D62 falls back into the allowed region in the semiquinone and hydroquinone structures. Plots of σ_A give estimated coordinate errors of 0.2, 0.21, and 0.25 Å for the D95A oxidized, semiquinone, and hydroquinone structures, respectively (*60*).

The models of the oxidized and hydroquinone forms of the D95E mutant also fit the final corresponding $2F_o - F_c$ electron density maps very well, although the density for residues 62−64 is weak at the 1σ level in both cases. Except for the main chain carbonyl of D63, all of the main chain

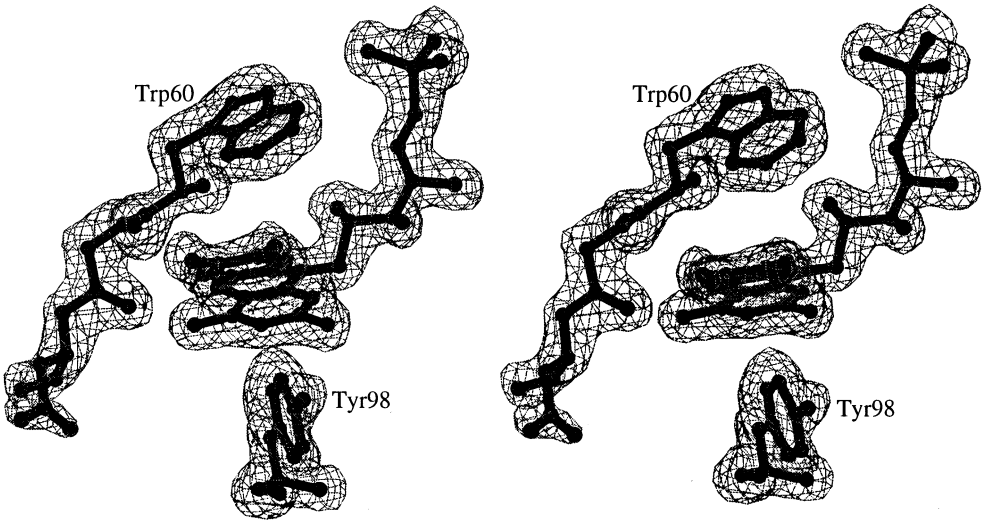

FIGURE 2: Stereoview of the final $2F_o - F_c$ electron density for W60−D62, Y98, and FMN of the D95A hydroquinone. The electron density is contoured at the 1.2σ level. This figure was produced with the programs BOBSCRIPT (*70*) and MOLSCRIPT (*71*).

atoms in the oxidized structure are clearly visible when the electron density is contoured at the 0.7σ level. Contouring at the same level for the electron density in the hydroquinone structure shows that all of the main chain atoms are clearly visible. The electron density for the D62 side chain is poor in both structures. The Ramachandran plot for the D95E oxidized structure shows that 95.2% of the residues lie in the most favored regions, 4.0% of the residues lie in additional allowed regions, and 0.8% are in generously allowed regions. None occur in the disallowed region. This is in contrast to the results for both the wild-type and D95A oxidized structures, where D62 is found in a disallowed region. The corresponding values for the D95E hydroquinone are 92.8% in the most favored regions and 7.2% in additionally allowed regions. The errors in positional coordinates as estimated from σ_A plots (*60*) are 0.15 and 0.22 Å for the D95E oxidized and hydroquinone forms, respectively.

Description of the Structures. The overall structure of *D. vulgaris* flavodoxin has been described in detail elsewhere (*7*, *34*, *61*). It consists of a central β-sheet surrounded by α-helices. The isoalloxazine ring is sandwiched between two aromatic residues located in loops at the C-terminus of the β-sheet (Figure 3). These β-turns are termed the "90-loop" and "60-loop". Residues 95−98 form a type I β-turn and flank the *si* or "outer" face of the isoalloxazine structure of the flavin, while residues 61−64 form a type II′ β-turn and flank the *re* or "inner" face of the isoalloxazine ring as classified with PROMOTIF (*63*).

Oxidized D95A Mutant Structure. The polypeptide chain conformations of the oxidized wild-type protein and the D95A mutant are almost identical, with some minor changes in the main chain and side chain conformations of D63, S64, and E66 (Table 4 and Figure 4). OE2 of residue E66 hydrogen bonds to OG of S64 in the wild-type structure at 120 K (*7*), but this is not observed in the wild-type structure at 293 K (*7*, *34*), where the E66 side chain is flexible. The D95 side chain makes hydrogen bonds to the main chain nitrogen of S97 and to OG of S97, stabilizing the 90-loop. The loss of these stabilizing hydrogen bonds in the 90-loop, as a result of the mutation, allows a concerted one-directional movement of the 90-loop, the FMN, and the 60-loop away from the body of the protein (0.2−0.3 Å for the main chain

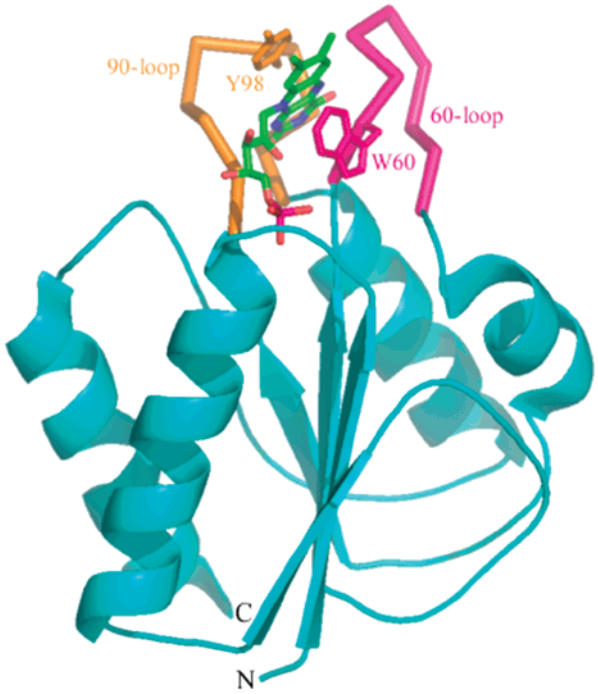

FIGURE 3: Ribbon diagram of flavodoxin highlighting the 60- and 90-loops that make up the isoalloxazine binding site of the FMN cofactor. The FMN and amino acid residues that sandwich the isoalloxazine are labeled and shown in ball-and-stick format.

atoms of the 90-loop, 0.1−0.3 Å for all non-hydrogen atoms of the FMN, and 0.3−1.18 Å for the main chain atoms of the 60-loop, with the largest displacement, 1.18 Å, occurring at S64 O). The E66 side chain movement is probably due to steric interactions between Cα of G61 and CG of E66 on the concerted movement of the 90-loop, the FMN, and the 60-loop. The movement of the E66 side chain allows a new orientation for the side chain of S64 and hence its new backbone conformation.

Reduced Structures of the D95A Mutant. The structural change on reduction of the D95A mutant to the semiquinone is similar to that seen in the wild-type flavodoxin. Some additional side chain rearrangements occur in the 60-loop of the D95A mutant semiquinone, relative to the structure of the semiquinone of the wild-type protein. The D62, D63,

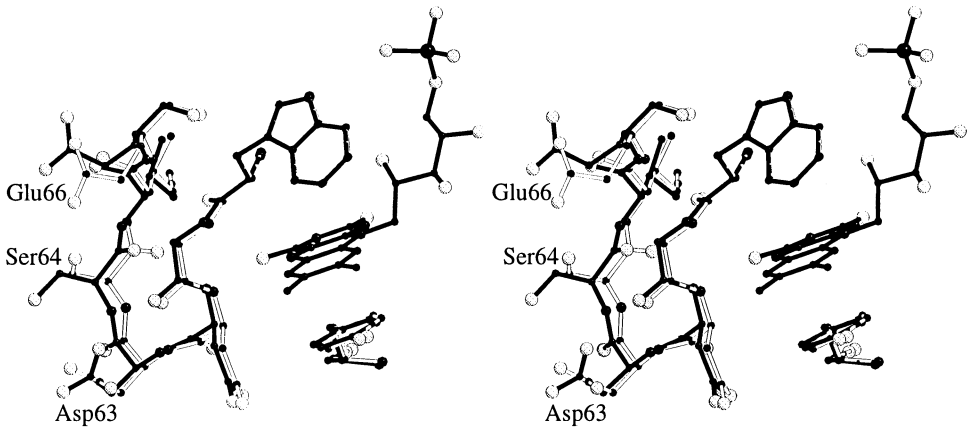

FIGURE 4: Stereoview of the superposition of the FMN binding site of oxidized wild-type (empty bonds) and oxidized D95A mutant (filled bonds) flavodoxins. Superposition using only Cα atoms not involved in FMN binding site. In this figure, oxygen atoms are drawn as empty circles. All other atoms are filled black, with radii increasing with atomic number. This figure was produced with the programs BOBSCRIPT (*70*) and MOLSCRIPT (*71*).

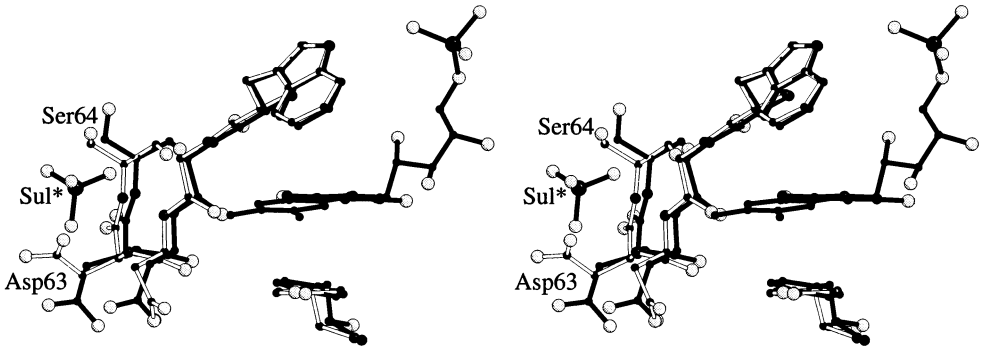

FIGURE 5: Stereoview of the superposition of the FMN binding site of semiquinone wild-type (empty bonds) and semiquinone D95A mutant (filled bonds) flavodoxins. Superposition using only Cα atoms not involved in FMN binding site. In this figure, oxygen atoms are drawn as empty circles. All other atoms are filled black, with radii increasing with atomic number. This figure was produced with the programs BOBSCRIPT (*70*) and MOLSCRIPT (*71*).

Table 4: Least-Squares Superpositions of the Structures of the D95A and D95E Mutant Proteins onto Wild-Type Flavodoxin

superposition	all Cα atoms	Cα atoms excluding those at the FMN binding site[a]
wt ox vs D95A ox	0.292	0.286
wt sq vs D95A sq	0.359	0.342
wt hq vs D95A hq	0.487	0.382
wt ox vs D95E ox	0.389	0.243
wt hq vs D95E ox	0.486	0.412

[a] Residues 10−15, 60−66, and 95−102.

and S64 side chains adopt new conformations by rotating away from the protein toward the solvent region (Figure 5). A sulfate or phosphate ion hydrogen bonds with the main chain nitrogens of D62 (2.94 Å), D63 (3.27 Å), and S64 (3.41 Å). This ion was not found in the wild-type semiquinone structure. The only other structural difference found is at the 90-loop where the Y98 phenol ring makes an angle of 12° with the FMN ring in the D95A semiquinone structure, relative to an angle of 4° in the wild-type protein.

On reduction to the hydroquinone, large conformational changes occur at residues 61−64 and 96−99 which is in contrast to wild-type flavodoxin in which no significant structural changes occur when the flavin is fully reduced (*7*; Table 4 and Figure 6). At the 90-loop, the side chain of Y98 is essentially flipped from a face-to-face interaction with the isoalloxazine ring to an edge-to-face interaction; the phenol ring of Y98 in the D95A mutant makes an angle of 74° with the isoalloxazine. To accommodate this rotation, a structural adjustment of residues 96−99 occurs, and this is accompanied by a movement of residues 61−64. The latter structural change does not disrupt the hydrogen bond from the carbonyl oxygen of G61 to the N(5)H group of the isoalloxazine moiety that is seen in the wild-type and D95A semiquinone. The structural rearrangement at the 60-loop introduces a kink in the loop at position 63 and causes the main chain atoms of this residue to be moved approximately 3 Å closer to the flavin. The structural adjustment is made possible by the space left by the rotation of the phenol ring side chain of Y98. This conformational change generates two new hydrogen bonds: one from the main chain nitrogen of E99 to OD1 of D63 (3.38 Å) and another mediated by water from OD2 of D63 to the main chain nitrogen of Y100. The sulfate or phosphate bound near the 60-loop in the semiquinone structure is not present in the hydroquinone structure. This could be due to the loss of favorable interactions with the 60-loop conformation in the hydroquinone structure. In addition to these changes, the space formed by the new orientation of the side chain of Y98 allows three further waters to bind at the FMN site.

Oxidized D95E Mutant Structure. The overall protein conformation of the D95E mutant is similar to that of wild-type flavodoxin except at the 60-loop (Table 4). In the native structure, the D62 nitrogen atom forms a weak hydrogen bond (3.49 Å) to N(5) of the flavin. It also forms a slightly

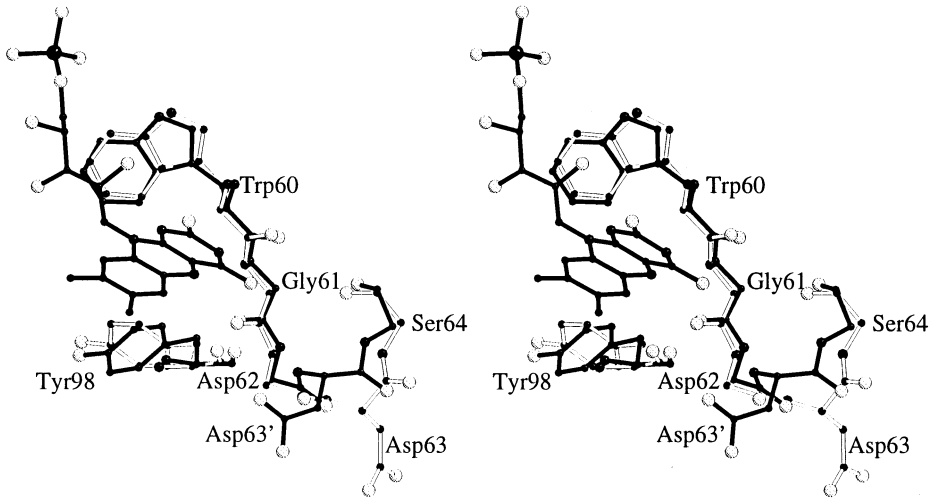

FIGURE 6: Stereoview of the superposition of the 60-loop and Y98 side chain of the wild-type flavodoxin (empty bonds) onto the 60-loop and Y98 side chain of the D95A hydroquinone mutant (filled bonds) using only Cα atoms not involved in FMN binding. Only the main chain atoms, except D63 and Y98, are shown for clarity. Residue labels for the D95A hydroquinone mutant are marked with an apostrophe. In this figure, oxygen atoms are drawn as empty circles. All other atoms are filled black, with radii increasing with atomic number. This figure was produced with the programs BOBSCRIPT (*70*) and MOLSCRIPT (*71*).

Table 5: Hydrogen Bonding Interactions between FMN and Protein Atoms in Oxidized *D. vulgaris* Wild-Type, D95A, and D95E Flavodoxins

		distance (Å)		
FMN atom	contact atom	wild type	D95A	D95E
O(2)	D/A/E95 N	3.08	3.03	3.07
	C102 N	2.78	2.81	2.79
N(3)	Y100 O	3.06	3.06	2.87
O(4)	D62 N	3.26	3.31	–
	wat O	2.75	2.76	2.83
	wat O	–	–	2.61
N(5)	D62 N	3.49	3.53	–
	wat O	–	–	3.32
O(2*)	T59 O	2.69	2.62	2.83
O(3*)	wat O	3.25	2.63	2.87
O(3*)	E95 OE2	–	–	3.50
O(4*)	D14 ND2	2.82	2.95	2.80
	wat O	2.65	2.53	2.62

stronger hydrogen bond (3.26 Å) to O(4) of the isoalloxazine moiety (Table 5). In the structure of the D95E mutant, the 60-loop has moved away from the flavin (Figure 7), adopting a conformation somewhat similar to the 60-loop in the apoflavodoxin−riboflavin complex (*29*). The largest displacement of a main chain atom in the 60-loop is for the main chain carbon of D62 (3.65 Å). The carbonyl oxygen of G61 now points toward the flavin binding site, whereas in the wild-type and D95A structures, it points away. This carbonyl oxygen forms a strong hydrogen bond (2.50 Å) to a water molecule (wat130) which in turn hydrogen bonds to O(4) and N(5) of FMN (2.61 and 3.32 Å, respectively; Table 5 and Figure 8). The carbonyl oxygen of S64 also hydrogen bonds to W130. The 60-loop projects into a solvent channel as a result of the different crystal packing observed in the D95E structure, whereas in the wild-type and D95A structures, it makes intermolecular hydrogen bonds. The loss of intermolecular contacts gives the 60-loop more flexibility in this mutant.

Apart from the mutation at position 95, the conformation of the 90-loop in this mutant is very similar to that of the wild-type structure. The loss of the hydrogen bonds formed by the carboxylate group of D95 to the main chain nitrogen and OG of S97 does not affect the conformation of this loop. OE2 of E95 makes a weak hydrogen bond to the O3* ribityl oxygen of FMN (3.5 Å) and does not hydrogen bond to the polypeptide main chain. The hydrogen bonding interactions of the main chain atoms of E95 are essentially identical to those in the wild-type structure. The introduction of the larger side chain at residue 95 results in a rotation and translation of the side chain of Y98 in the direction of the 60-loop, thus reducing the short van der Waals interactions between E95 OE1 and CE2 of Y98 (3.16 Å). Y98 CE1 and CZ are displaced by 0.54 and 0.44 Å, respectively. The isoalloxazine structure of the flavin also rotates toward the 60-loop, maintaining the $\pi-\pi$ interactions between the isoalloxazine and Y98. The C(7) atom of the flavin in this mutant is translated 0.92 Å relative to its position in the wild-type structure. The N(5) atom of the isoalloxazine is displaced by 0.65 Å. The pyrimidine rings of the isoalloxazines in the D95E mutant and wild-type structures are superimposable. The N(1), O(2), and N(3) atoms of the isoalloxazine hydrogen bond to the protein backbone as in the wild-type structure (Table 5).

Hydroquinone D95E Mutant Structure. A significant conformational change occurs in the 60-loop of D95E on reduction of the FMN to the hydroquinone, with the largest displacement occurring with the main chain oxygen of D62 (5.22 Å). The carbonyl oxygen of G61 moves closer to the protonated N(5)H nitrogen of the isoalloxazine structure to form a strong hydrogen bond (2.68 Å). This conformational change displaces the water molecule that mediates a hydrogen bond between these atoms in the oxidized form of the mutant protein. The conformational change is similar to that seen in the wild-type structures on reduction, with the result that the main chain conformation of the 60-loop in the hydroquinone of the mutant is similar to that of the hydroquinone of the wild-type protein (Figure 9). The D62 side chain adopts a different conformation in the D95E hydroquinone, but this side chain has poorly defined electron density. There is no conformational change in the main chain of the 90-loop, but the side chain of E95 adopts a new rotamer conformation on reduction, moving further away

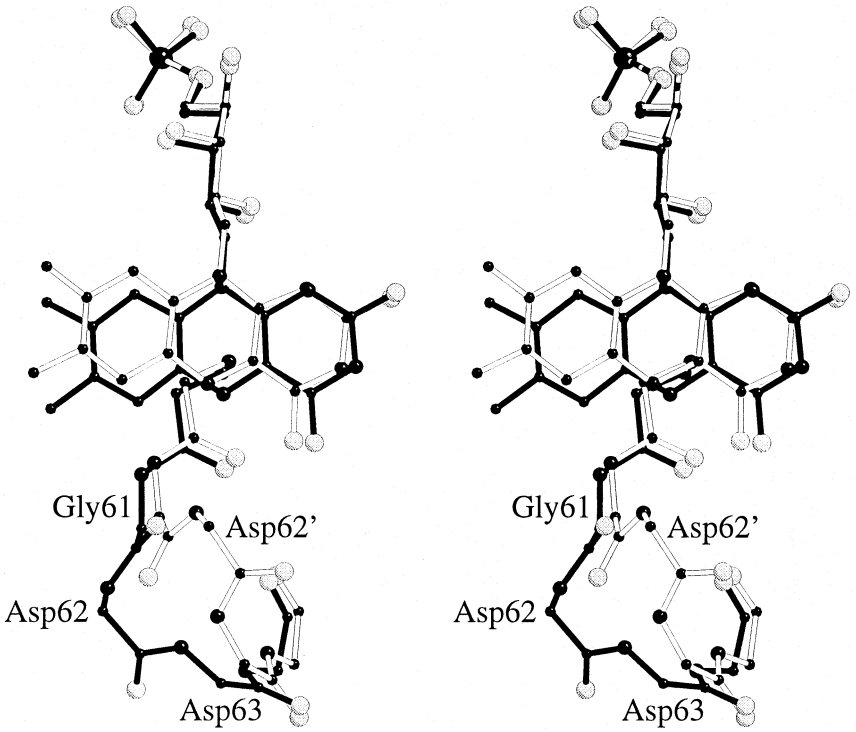

FIGURE 7: Stereoview of the superposition of the FMN binding site of oxidized wild-type (empty bonds) and oxidized D95E mutant (filled bonds) flavodoxins. Superposition using only Cα atoms not involved in FMN binding site. In this figure, oxygen atoms are drawn as empty circles. All other atoms are filled black, with radii increasing with atomic number. This figure was produced with the programs BOBSCRIPT (*70*) and MOLSCRIPT (*71*).

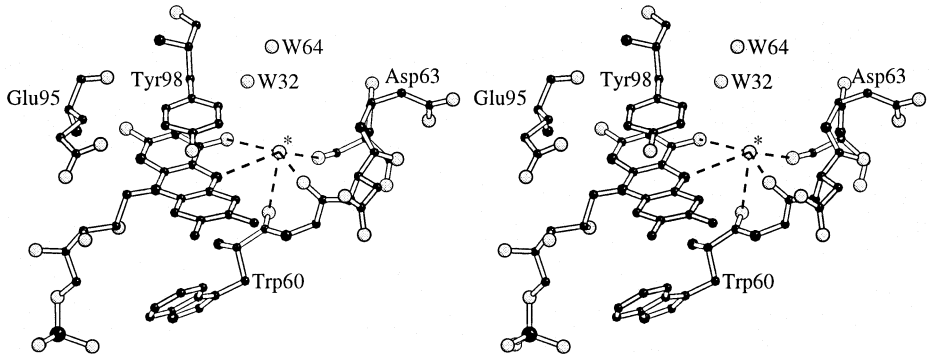

FIGURE 8: Stereoview of the FMN binding site in the oxidized D95E mutant flavodoxin. The hydrogen bonding interactions of the tightly bound water (indicated with an asterisk) are shown as dashed lines. In this figure, oxygen atoms are drawn as empty circles. All other atoms are filled black, with radii increasing with atomic number. This figure was produced with the programs BOBSCRIPT (*70*) and MOLSCRIPT (*71*).

from the isoalloxazine moiety and breaking the weak hydrogen bond to the O3* ribityl oxygen of the flavin.

Modeling of Protein−FMN Interactions. The conformational energies of the proteins (the FMN cofactor in its various oxidation states was excluded for these calculations) in each of the nine structures summarized in Table 6a show that the observed pattern of dissociation constants is well reflected qualitatively by the energetics of the changes in the protein conformations. The less stable FMN apoflavodoxin complexes are associated with protein conformations that are more strained in their respective binding modes. A complete correlation is not observed for several reasons, the main one being that while the calculations were carried out on one conformer, the dissociation constants refer to an average over a conformational ensemble. Analyses of the interaction energies of the flavin ring with the residues making up the binding site show that the destabilization of the hydroquinone relative to the semiquinone arises in part from the region of W60−E66 which contributes 1.5 kcal/mol (this would lead to a negative shift of 65 mV) and from G94−G103 which contributes 1.5−4.7 kcal/mol (this would lead to a negative shift of 130−200 mV). The free energy changes were calculated using the relationship

$$\delta\Delta G = -nF\,\delta E$$

where n is the number of electrons, F is Faraday's constant, and E is the redox potential.

In addition, we examined the internal energies of the flavin ligands in each oxidation state in both the bound and free forms (after optimization of their geometries). In the case of the semiquinone, the internal strain increases by 2 kcal/mol as the ligand goes into the bound state. In contrast, the hydroquinone state undergoes a destabilization of 8.4 kcal/mol that would lead to a shift in potential of ∼250 mV.

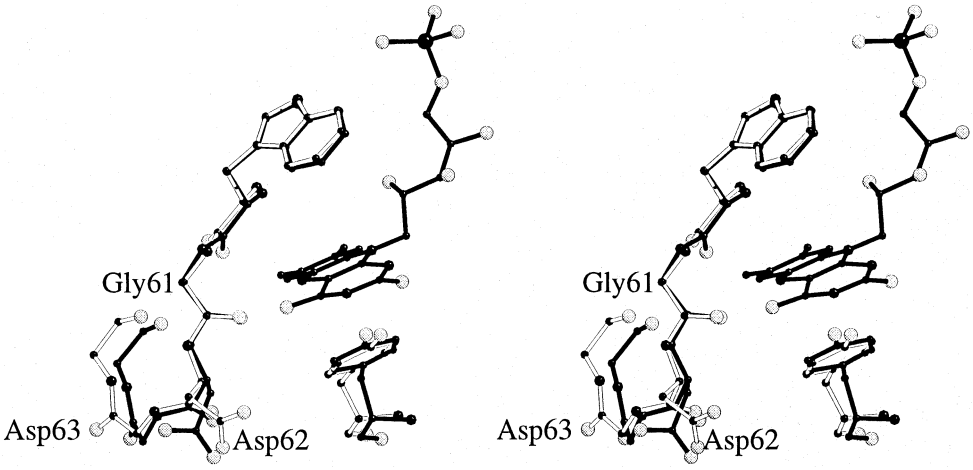

FIGURE 9: Stereoview of the superposition of the 60-loop and Y98 side chain of hydroquinone wild-type (empty bonds) and hydroquinone D95E mutant (filled bonds) flavodoxins using only Cα atoms not involved in FMN binding. Only the main chain atoms, except D62, Y98, and the mutation position, are shown for clarity. In this figure, oxygen atoms are drawn as empty circles. All other atoms are filled black, with radii increasing with atomic number. This figure was produced with the programs BOBSCRIPT (*70*) and MOLSCRIPT (*71*).

Table 6: Calculations Based on Molecular Modeling

(a) Relative Conformational Energies of the Protein When Bound to FMN[a]

protein	oxidized (kcal/mol)	semiquinone (kcal/mol)	hydroquinone (kcal/mol)
wild type	10.1	0	9.4
D95A	22.1	22.3	30.0
D95E	19.5	8.6	9.1

(b) Effects of Electrostatic Interactions of Selected Amino Acid Residues in the Proximity of FMN in Wild-Type, D95A, and D95E Flavodoxin Structures[b]

residue	wild-type $\delta\Delta G$[c]	D95A $\delta\Delta G$[c]	D95E $\delta\Delta G$[c]
D62	0.34 (−15)[d]	0.19 (−8)	0.30 (−13)
D63	0.10 (−4)	0.77 (−34)	0.12 (−5)
E66	0.17 (−7)	0.22 (−10)	0.25 (−11)
D95[e]	0.54 (−23)	−	0.6 (−26)
E99	0.13 (−6)	0.07 (−3)	0.17 (−7)
D106	0.22 (−10)	0.21 (−9)	0.25 (−11)
D127	0.22 (−10)	0.22 (−10)	0.30 (−13)

(c) Influence of Protein Electrostatics on FMN[f]

	$\delta\Delta G$ (kcal/mol)	ΔE_1 (mV)
wild type	2.6	−113
D95A	1.4	−61
D95E	0.9	−39

[a] Values are relative to the energy of the native semiquinone state which was the most stable conformation in the calculations; these energies are internal energies, δE, of each conformation and have been computed as E(holoprotein) − E(flavin in holoprotein). [b] The values are electrostatic free energies of interactions. [c] Electrostatic free energy difference between the semiquinone and hydroquinone states. [d] Equivalent contribution of the residue to the E_1 potential in millivolts. [e] Mutation site. [f] Electrostatic free energy of interaction between the semiquinone and hydroquinone states.

We further investigated how the E_1 potential is modulated by electrostatic interactions with charged amino acid side chains within a 15 Å sphere of the FMN binding site in all the reduced structures presented in this paper. Since the structure of the semiquinone of the D95E mutant was not determined, it was assumed to be similar to that of the fully reduced form (as is the case for the native flavodoxin structures determined to date). Table 6b lists the electrostatic free energy differences that were calculated between the semiquinone and the hydroquinone for the amino acids of interest in this study and the magnitude of the corresponding shift in the E_1 potential that these residues cause. While none of them individually have a significantly large contribution, together with the changes due to protein and ligand conformational energetics, they add up to the magnitudes of the changes observed experimentally. While these effects are small, other studies (*62*) have shown that Poisson−Boltzmann calculations can reproduce experimentally measured shifts in electrostatic properties (such as pK_a shifts) to an accuracy of greater than 94%. Analyses of the electrostatic free energy changes for the charged residues of the 60-loop highlight how the structural differences in the loop region affect the electrostatic interactions and hence the potentials. The wild type and E95 mutants have residues D62 and D63 in very similar conformations in their hydroquinone structures which is reflected in similar potentials. In the hydroquinone structure of the D95A mutant, D62 has moved closer to the flavin while D63 has moved further from the flavin, resulting in electrostatic effects that are the opposite of those of the wild type. The charged residues having the largest electrostatic effect on the flavin in the wild type are in the following order: D95 > D62 > D106/D127 > E66 > E99/D63. In all cases, the electrostatic contribution of Y98 (which is stacked against the *si*-face of the FMN) in the modulation of the FMN redox potential is less than 0.02 kcal/mol.

DISCUSSION

Electrostatic interactions at the flavin binding site have been shown to assist in modulating the redox properties of FMN in flavodoxin. In *D. vulgaris* flavodoxin, the closest charged amino acid to the N(1) atom of the isoalloxazine moiety is an aspartate residue at position 95 (D95). When this charged residue is neutralized in the asparagine mutant, the positive shift of the E1 potential that occurs is larger than when other nearby charged residues are neutralized (*25*, *32*). The crystal structure of this flavodoxin reveals that D95 forms part of a type I β-turn and that it contributes to the stability of this turn via hydrogen bonds through its carboxylate group to the amide nitrogen and OG of S97. Alignment of known flavodoxin sequences shows that aspartate is conserved in the long chain flavodoxins and that

in the structures determined to date, this aspartate is also found in the proximity of the flavin in a type I or type IV β-turn. To understand the role of D95 in the modulation of the bound FMN redox potentials, D95 has been mutated to alanine, asparagine, and glutamate. The mutant proteins have been biochemically characterized, and the crystal structures of the alanine and glutamate mutant flavodoxins have been determined in their oxidized and reduced states. These data allowed a detailed evaluation of the electrostatic interactions at the flavin binding site with particular emphasis on the role played by D95.

The D95A and D95E mutant proteins were successfully crystallized and yielded crystal structures of all three oxidation states in the case of the D95A mutant and structures of the oxidized and fully reduced forms of the D95E mutant. Although it is clear that the hydrogen bonds formed by D95 are eliminated by these mutations, the crystal structures of the oxidized forms show no notable structural changes at the mutation site. Structural changes were observed for the all of the reduced structures presented here. In the case of the D95A mutant is observed a conformational change at the 60-loop somewhat similar to that which occurs in the wild-type protein upon reduction to the semiquinone form. On reduction to the hydroquinone form, unexpected conformational changes are observed at both the 60- and 90-loops. In particular, the phenol ring side chain of Y98 is rotated by 74° around its CB−CG bond with respect to its structure in the oxidized state. The main consequence of this conformational change is that the phenol ring now makes an edge-to-face interaction with the flavin ring system instead of a face-to-face interaction. The face-to-face or aromatic stacking interaction that is observed in *D. vulgaris* flavodoxin between Y98 and the isoalloxazine moiety is a recurrent feature in other flavodoxins. This face-to-face interaction is unfavorable (*64*−*66*), and it has been suggested that it plays a significant role in the destabilization of the hydroquinone of the bound flavin (*27*). The unexpected structural change in the D95A mutant allows us to probe the importance of the aromatic stacking interaction in the modulation of the bound flavin's redox potentials.

Inspection of the E_1 value for this mutant (Table 3) shows it to be 16 mV less negative than that of wild-type flavodoxin. An assessment of the major contributions to the modulation of the E_1 redox potential based on the thermodynamic and structural data is complicated by the structural differences observed in the hydroquinone structures of the D95A mutant and wild-type structures at the 60-loop. However, derivation of the electrostatic interactions between the protein-bound FMN and individual amino acids based on the crystal structures allows the deconvolution of the major contributors to the modulation of the E_1 potential by electrostatic interactions. The conformational changes that occur on reduction of the semiquinone in the D95A mutant include residues in the 60-loop. Movement of D63 brings the charge on its side chain to 8.8 Å from N(1) of the flavin. At the same time, the carboxylate carbon of D62 is shifted 0.8 Å further away, while the positions of other charged residues in the vicinity of the flavin are more-or-less unchanged. The new positions of the side chains of D62 and D63 are likely to have opposite effects on the stability of the flavin hydroquinone.

Electrostatic calculations based on the crystal structures show that D62 in the D95A mutant destabilizes the hydroquinone state relative to the semiquinone with an electrostatic free energy change of 0.19 kcal/mol; the corresponding value for the wild-type protein is 0.34 kcal/mol (Table 6b). These effects are reversed in the wild-type and D95A mutant proteins for D63, which now has a stabilizing effect in the wild type when compared to its effect on the D95A hydroquinone (Table 6b). The net result of the conformational changes at the 60-loop in the D95A hydroquinone is that the unfavorable electrostatic interactions between D62 and D63 are increased by 0.52 kcal/mol which almost corresponds to the stabilization achieved by neutralization of D95 (0.54 kcal/mol, Table 6b).

Thus, in the D95A mutant, the expected stabilization of the hydroquinone form of the protein-bound FMN is effectively neutralized by the conformational changes that occur at the 60-loop. This implies that the 16 mV shift in E_1 of the D95A mutant can be attributed to a large extent to the other observed structural changes, namely, the elimination of the aromatic stacking interaction between the side chain of Y98 and the flavin, which also increases the solvent accessibility of the flavin by 10 Å^2 [as calculated using the standard 1.4 Å radius rolling sphere method (*67*)]. Analysis of the calculated overall influence of the electrostatic interactions in the wild-type and mutant flavodoxins with bound FMN (Table 6c) agrees with the trend observed experimentally.

Calculating the total contribution of individual charged amino acids to the destabilization of the hydroquinone in D95A implies that unfavorable aromatic stacking interactions in the wild-type protein perturb the E_1 potential negatively by at most 10 mV. Unraveling the exact contributions of aromatic stacking interactions and solvent exclusion is not straightforward without further structural data. Crystal structures of Y98 mutant flavodoxins might clarify the issues. Other preliminary results presented here show that on binding to the apoflavodoxin the hydroquinone form of FMN is under far more internal strain than is the case for the FMN semiquinone. Calculation of the total energies of the free and bound oxidation states of FMN shows that the D95A hydroquinone is subjected to approximately 3 kcal/mol less strain than the wild-type structure. The increased level of solvent exposure of the hydroquinone and the now edge-to-face interaction with the phenol ring of Y98 can be inferred to play a role in the decrease. It should be noted that these calculations are very sensitive to atomic positions and thus provide only an indication of the forces at play.

The structural changes caused by mutation of D95 to glutamate do not include rotation of the Y98 phenol ring when the mutant is fully reduced; the ring remains coplanar with the isoalloxazine moiety. The rotamer conformation of the E95 side chain in the reduced form of this mutant is different. It seemed possible that this change in conformation might prevent the Y98 side chain from undergoing the rotation seen with the D95A mutant. However, analysis of all possible rotamers of the E95 side chain showed that none restrict the rotation of the phenol ring of Y98. Therefore, steric restraints cannot be invoked to explain the structural results for the D95E mutant. It is possible that the degree of electrostatic repulsion between the carboxylate of the glutamate and the phenol ring of Y98 is greater than the corresponding

degree of electrostatic repulsion between the phenol ring and the isoalloxazine. This interaction sustains the unfavorable face-to-face conformation of the two ring systems seen in the D95E mutant protein. A similar explanation could account for the unfavorable stacking interaction of the Y98 phenol ring and flavin in the wild-type protein. In this case, the carboxylate group is provided by D95. Support for this hypothesis comes from the observation that cations are strongly attracted to the π-face of aromatic structures. The magnitude of this noncovalent cation $\pi-\pi$ interaction depends largely on the nature of the ion, but it can be as high as 38 kcal/mol (*68*).

The relative contribution of D95 to the stability of the 90-loop through hydrogen bonding interactions can be assessed from the values of the conformational energies of the various oxidation states of the flavodoxin structures that were determined (Table 6a). The values agree with the trend observed experimentally with the D95A hydroquinone being the least stable complex. In both the D95A and D95E mutants, the hydrogen bonds formed by the D95 side chain are eliminated. The structural basis for the weaker binding of FMN in the three oxidation states of the D95A mutant appears to be highly dependent on the small changes in the hydrogen bonding interactions that occur in the 60- and 90-loops, which form the isoalloxazine binding site for the FMN. The movements of the 60- and 90-loops in the D95A mutant with respect to the wild-type protein weaken the protein hydrogen bonds to FMN (Table 5). The loss of D95 has a significant effect on the stability of the flavodoxin structures for all oxidation states, as shown in Table 6a. The significantly weaker binding of FMN to the D95A mutant, especially in the semiquinone form, highlights the important role D95 plays in the binding of the FMN cofactor.

The dissociation constants for the oxidized FMN in wild-type and D95E mutant proteins are similar. Although there is a conformational change in the 60-loop of the D95E mutant, the reorganization of the hydrogen bonding network at the FMN binding site compensates for the change in structure. In the oxidized D95E mutant structure, the rotation of the flavin results in a lengthening of the hydrogen bond (0.19 Å) between Y100 O and N(3), but this is compensated by a strengthened hydrogen bond between T59 O and O(2*) (0.14 Å shorter than in the wild-type protein). Two direct hydrogen bonds to the FMN are lost due to the conformational change of the 60-loop in the D95E mutant, although the hydrogen bond between D61 N and N(5) of the flavin is weak or does not occur (*33*). The loss of the hydrogen bond between D62 N and O(4) of the flavin is replaced by a water-mediated hydrogen bond to W60 O, G61 O, and Ser64 O, and a new hydrogen bond between the side chain of E95 and O(3*) of FMN.

In conclusion, our results suggest that D95 in *D. vulgaris* flavodoxin has a dual function in modulating the redox properties of bound FMN. It has a direct effect through an unfavorable electrostatic interaction with the negatively charged hydroquinone of the flavin. It also interacts electrostatically with the phenol ring of Y98, and in this way prevents the favorable rotation of the phenol ring to an edge-to-face orientation with the isoalloxazine moiety. Similar roles can be inferred for other flavodoxins in which this aspartate is conserved.

ACKNOWLEDGMENT

M.A.W. thanks Keith S. Wilson for providing an excellent environment at the EMBL outstation Hamburg for carrying out this work.

REFERENCES

1. Mayhew, S. G., and Ludwig, M. L. (1975) in *The Enzymes* (Boyer, P. D., Ed.) 3rd ed., Vol. 12B, pp 57−109, Academic Press, New York.
2. Mayhew, S. G., and Tollin, G. (1992) in *Chemistry and Biochemistry of Flavoenzymes* (Müller, F., Ed.) Vol. 3, pp 389−426, CRC Press, Boca Raton, FL.
3. Ludwig, M. L., and Luschinsky, C. L. (1992) in *Chemistry and Biochemistry of Flavoenzymes* (Müller, F., Ed.) Vol. 3, pp 427−466, CRC Press, Boca Raton, FL.
4. Burnett, R. M., Darling, G. D., Kendall, D. S., Le Quesne, M. E., Mayhew, S. G., Smith, W. W., and Ludwig, M. L. (1974) *J. Biol. Chem. 249*, 4385−4392.
5. Sharkey, C., Mayhew, S. G., Higgins, T. M., and Walsh, M. A. (1997) in *Flavins and Flavoproteins 1996* (Stevenson, K. J., Massey, V., and Williams, C. H., Jr., Eds.) pp 445−448, University of Calgary Press, Calgary.
6. van Mierlo, C. P. M., Lijnzaad, P., Veervoort, J., Müller, F., Berendsen, H. J. C., and de Vlieg, J. (1990) *Eur. J. Biochem. 194*, 185−198.
7. Watt, W., Tulinsky, A., Swenson, R. P., and Watenpaugh, K. D. (1991) *J. Mol. Biol. 218*, 195−208.
8. Smith, W. W., Pattridge, K. A., Ludwig M. L., Petsko, G. A., Tsernoglou, D., Tanaka, M., and Yasunobu, K. T. (1983) *J. Mol. Biol. 165*, 737−753.
9. Hoover, D. M., and Ludwig, M. L. (1997) *Protein Sci. 6*, 2525−2537.
10. Rao, S. T., Shaffie, F., Yu, C., Satyshur, K. A., Stockman, B. J., Markley, J. L., and Sundarlingham, M. (1992) *Protein Sci. 1*, 1413−1427.
11. Romero, A., Caldiera, J., LeGall, J., Moura, I., Moura, J. J. G., and Romao, M. J. (1996) *Eur. J. Biochem. 239*, 190−196.
12. Fukuyama, K., Matsubara, H., and Rogers, L. J. (1992) *J. Mol. Biol. 225*, 775−789.
13. Smith, W. W., Burnett, R. M., Darling, G. D., and Ludwig, M. L. (1977) *J. Mol. Biol. 117*, 195−225.
14. Ludwig, M. L., and Luschinsky, C. L. (1992) in *Chemistry and Biochemistry of Flavoenzymes* (Müller, F., Ed.) Vol. 3, pp 427−466, CRC Press, Boca Raton, FL.
15. Luschinsky, C. L., Dunham, W. R., Osborne, K. A., Pattridge, K. A., and Ludwig, M. L. (1992) in *Flavins and Flavoproteins 1991* (Curti, B., Ronchi, S., and Zanetti, G., Eds.) pp 409−414, de Gruyter, Berlin.
16. Ludwig, M. L., Pattridge, K. A., Metzger, A. L., Dixon, M. M., Eren, M., Feng, Y., and Swenson, R. P. (1997) *Biochemistry 36*, 1259−1280.
17. Kasim, M., and Swenson, R. P. (2000) *Biochemistry 39*, 15322−15332.
18. Moonen, C. T. W., Vervoort, J., and Müller, F. (1984) *Biochemistry 23*, 4859−4867.
19. Zheng, Y., and Ornstein, R. L. (1996) *J. Am. Chem. Soc. 118*, 9402−9408.
20. Rizzo, C. J. (2001) *Antioxid. Redox Signaling 3*, 737−746.
21. Ludwig, M. L., Schopfer, L. M., Metzger, A. L., Pattridge, K. A., and Massey, V. (1990) *Biochemistry 29*, 10364−10375.
22. Franken, H.-D., Reterjans, H., and Müller, F. (1984) *Eur. J. Biochem. 138*, 481−489.
23. Vervoort, J., Müller, F., Mayhew, S. G., van den Berg, W. A. M., Moonen, C. T. W., and Bacher, A. (1986) *Biochemistry 25*, 6789−6799.
24. Swenson, R. P., and Krey, G. D. (1994) *Biochemistry 33*, 8505−8514.
25. Zhou, Z., and Swenson, R. P. (1995) *Biochemistry 34*, 3183−3192.
26. Zhou, Z., and Swenson, R. P. (1996) *Biochemistry 35*, 12443−12454.
27. Zhou, Z., and Swenson, R. P. (1996) *Biochemistry 35*, 15980−15988.
28. Moonen, C., Vervoort, J., and Müller, F. (1984) in *Flavins and Flavoproteins 1983* (Bray, R. C., Engel, P. C., and Mayhew, S. G., Eds.) pp 493−496, de Gruyter, Berlin.

29. Walsh, M. A., McCarthy, A., O'Farrell, P. A., McArdle, P., Cunningham, P. D., Mayhew, S. G., and Higgins, T. M. (1998) *Eur. J. Biochem. 258*, 362−371.
30. Yalloway, G. N., Mayhew, S. G., Malthouse, J. P. G., Gallagher, M. E., and Curley, G. P. (1999) *Biochemistry 38*, 3753−3762.
31. Yalloway, G. N., Mayhew, S. G., Boren, S. J., and Vervoort, J. (1999) in *Flavins and Flavoproteins 1999* (Ghisla, S., Kroneck, P., Macheroux, P., and Sund, H., Eds.) pp 187−190, Rudolf Weber, Berlin.
32. Mayhew, S. G., O'Connell, D. P., O'Farrell, P. A., Yalloway, G. N., and Geoghegan, S. M. (1996) *Biochem. Soc. Trans. 24*, 122−127.
33. O'Farrell, P. A., Walsh, M. A., McCarthy, A. A., Higgins, T. M., Voordouw, G., and Mayhew, S. G. (1998) *Biochemistry 37*, 8405−8416.
34. Walsh, M. A. (1994) Ph.D. Thesis, National University of Ireland, Galway, Ireland.
35. Mayhew, S. G. (1978) *Eur. J. Biochem. 85*, 535−547.
36. Otwinowski, Z., and Minor, W. (1997) *Methods Enzymol. 276*, 273−278.
37. Navaza, J. (1994) *Acta Crystallogr. D50*, 157−163.
38. Jones, T. A., Zou, J. Y., Cowan, S. W., and Kjeldgaard, M. (1991) *Acta Crystallogr. A47*, 110−119.
39. Collaborative Computational Project, No. 4 (1994) *Acta Crystallogr. D50*, 760−763.
40. Lamzin, V. S., and Wilson, K. S. (1997) *Methods Enzymol. 277*, 269−305.
41. Brooks, B. R., Bruccoleri, R. E., Olafson, B. D., States, D. J., Swaminathan, S., and Karplus, M. (1983) *J. Comput. Chem. 4*, 187−217.
42. Brzozowski, A. M., Savage, H., Verma, C. S., Turkenberg, J. P., Lawson, D. M., Svendsen, A., and Patkar, S. (2000) *Biochemistry 39*, 15071−15082.
43. Baerends, E. J., Ellis, D. E., and Ros, P. (1973) *J. Chem. Phys. 2*, 42−51.
44. Versluis, L., and Ziegler, T. J. (1988) *J. Chem. Phys. 88*, 322−398.
45. Velde, G. T., and Baerends, E. J. (1992) *J. Comput. Phys. 99*, 84−98.
46. Guerra, C. F., Snijders, J. G., te Velde, G., and Baerends, E. J. (1998) *Theor. Chem. Acc. 99*, 391−403.
47. Vosko, S. H., Wilk, L., and Nusair, M. (1980) *Can. J. Phys. 58*, 1200−1211.
48. Becke, A. D. (1988) *Phys. Rev. A 38*, 3098−3100.
49. Lee, C., Yang, W., and Parr, R. G. (1988) *Phys. Rev. B 37*, 785−789.
50. MacKerell, A. D., Bashford, D., Jr., Bellott, M., Dunbrack, R. L., Evanseck, J. D., Field, M. J., Fischer, S., Gao, J., Has, S., Joseph-McCarthy, D., Kuchnir, L., Kuczera, K., Lau, F. T. K., III, Mattos, C., Michnik, S., Ngo, S., Nguyen, D. T., Prodhom, B., Reiher, W. E., Roux, B., Schlenkrich, M., Smith, J. C., Stole, R., Strub, J., Watanabe, M., Wiorkiewicz-Kuczera, J., Yin, D., and Karplus, M. J. (1998) *J. Phys. Chem. B 102*, 3586−3616.
51. Davis, M. E., Madura, J. D., Sines, J., Luty, B. A., Allsion, S. A., and McCammon, J. A. (1991) *Methods Enzymol. 202*, 473−497.
52. Madura, J. D., Briggs, J. M., Wade, R. C., Davis, M. E., Luty, B. A., Ilin, A., Antosiewicz, J., Gilson, M. K., Bagheri, B., Scott, L. R., and McCammon, J. A. (1995) *Comput. Phys. Commun. 91*, 57−95.
53. Antosiewicz, J., McCammon, J. A., and Gilson, M. K. (1994) *J. Mol. Biol. 238*, 415−436.
54. Gilson, M. K., Davis, M. E., Luty, B. A., and McCammon, J. A. (1993) *J. Phys. Chem. 97*, 3591−3600.
55. Yang, A. S., and Honig, B. (1993) *Proteins*: *Struct., Funct., Genet. 15*, 252−265.
56. Curley, G. P., Carr, M. C., Mayhew, S. G., and Voordouw, G. (1991) *Eur. J. Biochem. 202*, 1091−1100.
57. Anderson, R. F. (1983) *Biochim. Biophys. Acta 772*, 158−162.
58. Mayhew, S. G. (1999) *Eur. J. Biochem. 265*, 698−702.
59. Ramachandran, G. N., and Sasisekharan, V. (1968) *Adv. Protein Chem. 23*, 283−437.
60. Read, R. J. (1986) *Acta Crystallogr. A42*, 140−149.
61. Watenpaugh, K. D., Sieker, L. C., and Jensen, L. H. (1973) *Proc. Natl. Acad. Sci. U.S.A. 70*, 3857−3860.
62. Pinitglang, S., Watts, A. B., Patel, M., Reid, J. D., Noble, M. A., Gul, S., Bokth, A., Naeem, A., Patel, H., Thomas, E. W., Sreedharan, S. K., Verma, C., and Brocklehurst, K. (1997) *Biochemistry 36*, 9968−9982.
63. Hutchinson, E. G., and Thornton, J. M. (1996) *Protein Sci. 5*, 212−220.
64. Burley, S. K., and Petsko, G. A. (1985) *Science 229*, 23−28.
65. Hunter, C. A., and Sanders, J. K. M. (1990) *J. Am. Chem. Soc. 112*, 5525−5534.
66. Hunter, C. A., Singh, J., and Thornton, J. M. (1991) *J. Mol. Biol. 218*, 837−846.
67. Connolly, M. L. (1983) *Science* 221, 709−712.
68. Dougherty, D. A. (1996) *Science 271*, 163−168.
69. Brunger, A. T. (1992) *Nature 355*, 472−475.
70. Esnouf, R. M. (1997) *J. Mol. Graphics Modell. 15*, 132−134.
71. Kraulis, P. J. (1991) *J. Appl. Crystallogr. 24*, 946−950.

BI020225H